

## *In-situ* preparation of Al matrix composites reinforced by TiB<sub>2</sub> particles and sub-micron ZrB<sub>2</sub>

DEGANG ZHAO\*, XIANGFA LIU, YUXIAN LIU, XIUFANG BIAN

The Key Laboratory of Materials Liquid Structure and Heredity, Ministry of Education, Shandong University, Jinan 250061, P. R. China  
E-mail: degang2008@163.com

Particulate-reinforced metal-matrix composites (PRMMCs) are of particular interest due to their ease of fabrication, low costs and isotropic [1]. The selection of a compatible reinforcement is very important for PRMMCs. Among various reinforcements used in the PRMMCs such as TiC, TiB<sub>2</sub>, Al<sub>2</sub>O<sub>3</sub>, SiC, ZrB<sub>2</sub> and BN, TiB<sub>2</sub> and ZrB<sub>2</sub> are excellent reinforcements. This is due to the fact that TiB<sub>2</sub> and ZrB<sub>2</sub> are stiff, hard and more importantly, do not react with aluminum to form any reaction products [2]. There are many reports about the fabrications and mechanical behaviors about TiB<sub>2</sub>/Al composites [3–6]; however, information related to the synthesis of composites with combined *in-situ* TiB<sub>2</sub> and ZrB<sub>2</sub> is very limited. In this paper, a novel Al matrix composite reinforced with TiB<sub>2</sub> and ZrB<sub>2</sub> was fabricated by the mixing salts reaction method and the microstructures of the composites were investigated with scanning electron microscope (SEM) and transmission electron microscope (TEM). X-ray diffraction (XRD) was used to identify the phases in the composites.

The composites were fabricated by mixing salts reaction process at 860 °C with KBF<sub>4</sub>, K<sub>2</sub>ZrF<sub>6</sub> and K<sub>2</sub>TiF<sub>6</sub> salts used. The 99.85% commercial pure Al was first melted in clay-graphite crucible using an intermediate frequency furnace at 800 °C, after which a pre-

weighted mixture of KBF<sub>4</sub>, K<sub>2</sub>ZrF<sub>6</sub> and K<sub>2</sub>TiF<sub>6</sub> (the weight ratio of KBF<sub>4</sub>:K<sub>2</sub>ZrF<sub>6</sub>:K<sub>2</sub>TiF<sub>6</sub>:Al is 7:12:8:73) was added into the molten metal using the stirring method at 860 °C. Then the melt was stirred for 10–15 min and *in-situ* TiB<sub>2</sub> and ZrB<sub>2</sub> particles were formed in the melt as the resultants of chemical reactions among the three salts and Al. After pouring out the liquid slag (fluoride), the melt was cast into the rods of 25 mm diameter. The samples for microstructure observations and XRD analysis were cut from the bulk of ingots. The samples were metallographically prepared using conventional grinding and mechanical polishing techniques. The TEM samples were initially polished to 100 μm in thickness using the SiC paper. Then 3 mm disc samples were punched from these thinned samples and ground to a thickness of 20 μm. Finally, the disc samples were thinned by argon ion milling (Gatan) with an incident angle of 10 ° until a perforation occurred.

The formations of TiB<sub>2</sub> and ZrB<sub>2</sub> reinforcements via the potassium fluoride molten salts mixture are thermodynamically favorable. The overall reaction is divided into two steps: (a) the reactions among KBF<sub>4</sub>, K<sub>2</sub>ZrF<sub>6</sub>, K<sub>2</sub>TiF<sub>6</sub> salts and Al; (b) resultants of former reaction continue to react to produce the TiB<sub>2</sub> and ZrB<sub>2</sub> phases. Table I shows the values of the Gibbs free energy of all

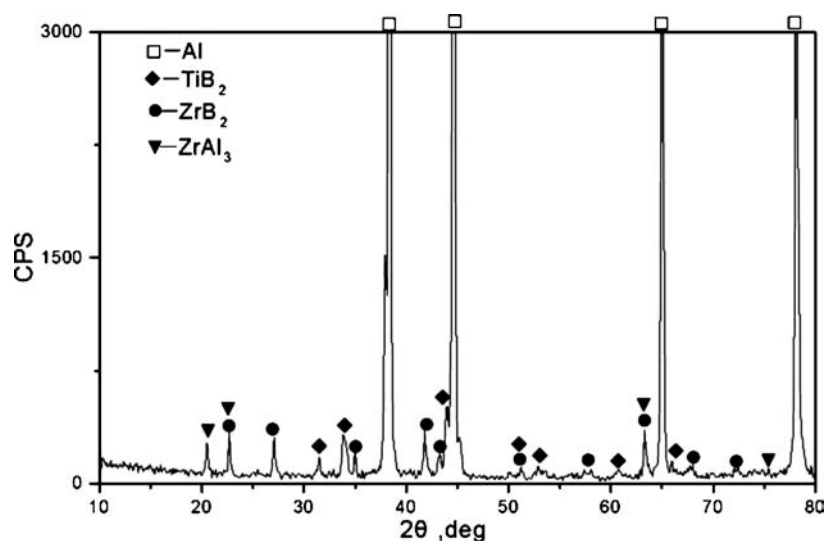


Figure 1 X-ray diffraction patterns of (TiB<sub>2</sub> + ZrB<sub>2</sub>)/Al composites.

\*Author to whom all correspondence should be addressed.

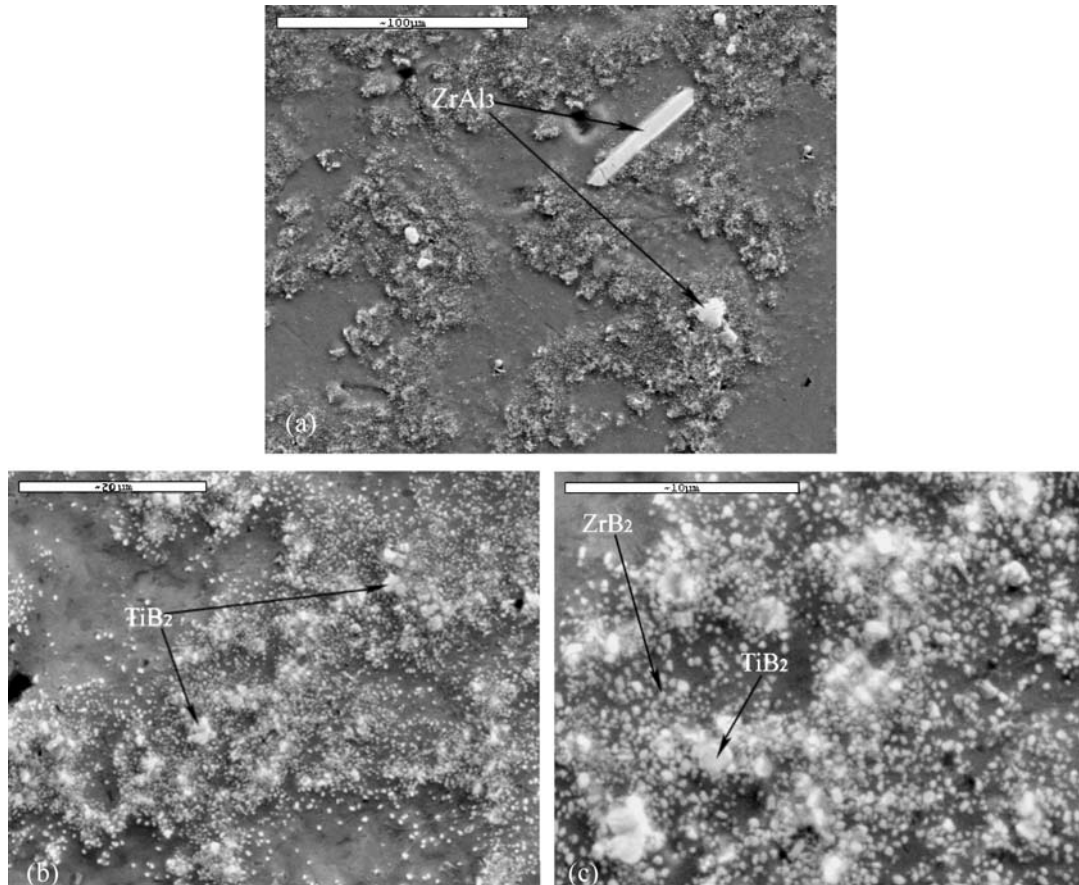
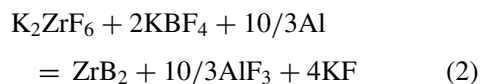
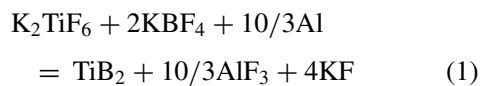


Figure 2 (a, b) SEM micrograph of the (TiB<sub>2</sub> + ZrB<sub>2</sub>)/Al composites (c) enlarged graph corresponding to (b).

reactions at 1000 K [7]. The overall reactions showing the formations of TiB<sub>2</sub> and ZrB<sub>2</sub> can be written as:



From the reactions shown in Table I, the Gibbs free energy values of reaction (1) and (2) are  $-860.08$  and  $-758.53$  KJ/mol, respectively. Both of them are exothermic reactions and are favorable at about 1000 K.

Fig. 1 shows the XRD (using Cu-K $\alpha$  radiation and operating at 40 kV and 100 mA) patterns of (ZrB<sub>2</sub> + TiB<sub>2</sub>)/Al composites. It indicates that the present phases in the composite are  $\alpha$ -Al, TiB<sub>2</sub>, ZrB<sub>2</sub>, and ZrAl<sub>3</sub>. The result of the XRD analysis confirms that Al matrix com-

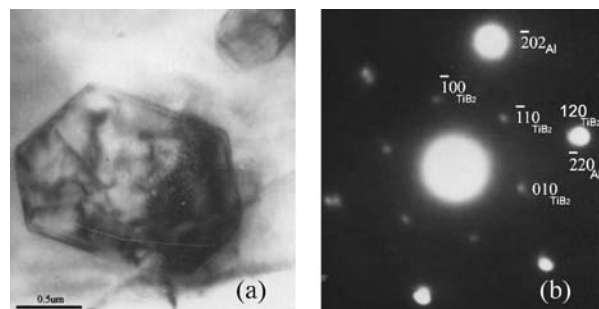


Figure 3 (a) TEM image of TiB<sub>2</sub> (b) composite electron diffraction patterns from TiB<sub>2</sub> crystal axis along [001] and Al along [111].

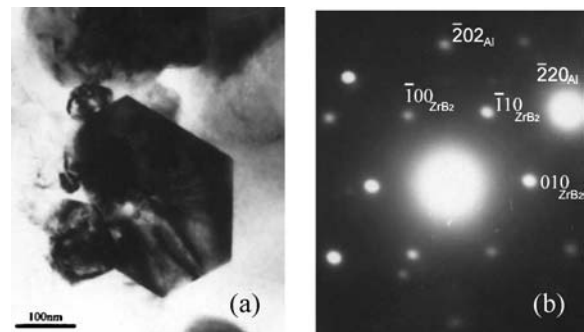


Figure 4 TEM image of ZrB<sub>2</sub> (b) composite electron diffraction patterns from ZrB<sub>2</sub> crystal axis along [001] and Al along [111].

TABLE I The reactions and the standard Gibbs free energy values at 1000 K

Reactions	$\Delta G^\circ$ (KJ/mol) 1000 K
(i) $2\text{KBF}_4 + 3\text{Al} = \text{AlB}_2 + 2\text{AlF}_3 + 2\text{KF}$	-404.31
(ii) $\text{K}_2\text{TiF}_6 + 13/3\text{Al} = \text{TiAl}_3 + 4/3\text{AlF}_3 + 2\text{KF}$	-354.65
(iii) $\text{K}_2\text{ZrF}_6 + 13/3\text{Al} = \text{ZrAl}_3 + 4/3\text{AlF}_3 + 2\text{KF}$	-276.24
(iv) $\text{TiAl}_3 + \text{AlB}_2 = \text{TiB}_2 + 4\text{Al}$	-101.12
(v) $\text{ZrAl}_3 + \text{AlB}_2 = \text{ZrB}_2 + 4\text{Al}$	-77.98

posites reinforced with TiB<sub>2</sub> and ZrB<sub>2</sub> particles can be fabricated by the mixing salts reaction process. SEM micrographs of (ZrB<sub>2</sub> + TiB<sub>2</sub>)/Al composite are presented in Fig. 2. From the Fig. 2a and b it can be seen

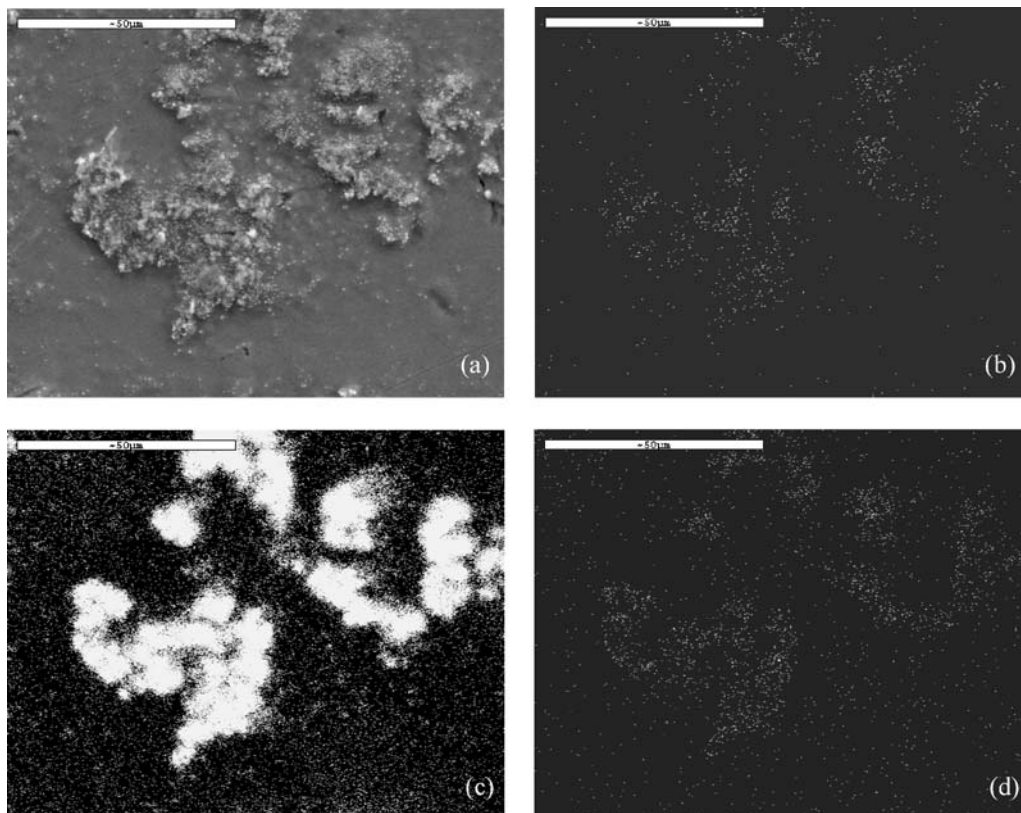


Figure 5 EPMA elemental of  $(\text{TiB}_2 + \text{ZrB}_2)/\text{Al}$  composites (a) SEM micrograph and X-ray dot maps of element; (b) B; (c) Ti; (d) Zr.

that most of the  $\text{TiB}_2$  and  $\text{ZrB}_2$  particles are distributed along the grain boundary regions and some agglomerations (clusters) of the particles are observed. The distribution of particles is not homogeneous in the Al matrix; however, the agglomerations or clusters, distribute uniformly. The average size of agglomerations (clusters) is  $40\text{--}50\ \mu\text{m}$ . The results of energy dispersion X-ray (EDX) spectrometer indicate the bigger reinforcements in Fig. 2c are  $\text{TiB}_2$  particles, while the smaller ones are  $\text{ZrB}_2$  phases. The  $\text{ZrB}_2$  reinforcements distribute around the  $\text{TiB}_2$  reinforcements. The main reason for agglomeration of particles is that the ratios of heat transfer coefficient between the particle reinforcements and matrix are less than 1. According to the theory of thermal conductivity in the process of solidification, the  $\text{TiB}_2$  and  $\text{ZrB}_2$  reinforcements are pushed by the solidification front. As a result, the  $\text{TiB}_2$  and  $\text{ZrB}_2$  particles agglomerate at the solid/liquid interface during solidification. In addition, it also can be found that there are some strip-shaped phase and near-spherical phase existing in the composites as shown in Fig. 2a. With the help of EDX, it can be concluded that they are all  $\text{ZrAl}_3$  phases, which are also present in the XRD result. The main reason for the formation of  $\text{ZrAl}_3$  phase is that chemical reaction (2) is incomplete. If the atomic ratio of  $\text{Ti}/2\text{B}$  and  $\text{Zr}/2\text{B}$  is controlled strictly and reaction holding time is longer, the  $\text{ZrAl}_3$  phase will tend to decompose to form  $\text{ZrB}_2$ . The  $\text{TiAl}_3$  phase is not observed because the atom ratio of  $\text{Ti}:\text{B}$  in the salts mixture is less than 1:2.

Figs 3 and 4 show the typical bright field TEM images of reinforcements and the composite electron diffraction patterns of reinforcements and matrix. It can be

observed that the  $\text{TiB}_2$  and  $\text{ZrB}_2$  particles are hexagonal and near-equiaxed shape, but  $\text{TiB}_2$  particles are bigger than  $\text{ZrB}_2$  particles in size. The average size of  $\text{TiB}_2$  particle is  $1\text{--}1.20\ \mu\text{m}$ , while that of  $\text{ZrB}_2$  particle belongs to sub-micron size and is about  $0.30\ \mu\text{m}$ . From Fig. 5a and d, which show the EPMA micrographs of agglomerations (clusters) in the composites and X-ray dot maps of elements B, Zr, Ti, it can be observed that the distributions of Ti, Zr and B elements are coincident on the whole.

The shape of the reinforcements is related to their crystal structures.  $\text{TiB}_2$  or  $\text{ZrB}_2$  particle has a  $\text{C32-A1B}_2$  structure and  $\text{MeB}_2$  type ( $\text{TiB}_2$  with lattice parameters  $a = 0.3029\ \text{nm}$ ,  $c = 0.3228\ \text{nm}$ ;  $\text{ZrB}_2$  with lattice parameters  $a = 0.317\ \text{nm}$ ,  $c = 0.3513\ \text{nm}$ ). The crystal structure of  $\text{TiB}_2$  or  $\text{ZrB}_2$  shows high geometrical symmetry for the chemical bond between the atoms Ti (or Zr) and B. This indicates that  $\text{TiB}_2$  or  $\text{ZrB}_2$  will grow almost at the same speed in each direction and form equiaxed or near equiaxed shape.

In conclusion, our results show that *in situ*  $(\text{ZrB}_2 + \text{TiB}_2)/\text{Al}$  composites were synthesized successfully through the mixing salts reaction among the  $\text{KBF}_4$ ,  $\text{K}_2\text{ZrF}_6$ ,  $\text{K}_2\text{TiF}_6$  and Al. The agglomerations (clusters) of the particles distribute uniformly in the Al matrix. The  $\text{TiB}_2$  and  $\text{ZrB}_2$  particles are hexagonal and near-equiaxed shape. The average size of  $\text{TiB}_2$  particle is about  $1\ \mu\text{m}$  while that of  $\text{ZrB}_2$  particle is about  $0.30\ \mu\text{m}$ .

#### Acknowledgments

The authors are very grateful for the support of Natural Science Foundation of China (No. 50171037), and

the support of the Key Project of Science and Technology Research of Ministry of Education of China (No. 01105).

### References

1. M. S. THOMPSON and V. C. NARDONE, *Mater. Sci. Eng. A* **144** (1991) 121.
2. S. C. TIONG and Z. Y. MA, *ibid.* **29** (2000) 9.
3. G. J. ZHANG, M. ANDO, J. F. YANG and T. OHJI, *J. Eur. Ceram. Soc.* **24** (2004) 171.
4. K. L. TEE, L. LU and M. O. LAI, *Composite Struct.* **47** (1999) 589.
5. Y. F. HAN, X. F. LIU and X. F. BIAN, *Compos. Part A* **33** (2002) 439.
6. S. LAKSHMI, L. LU and M. GUPTA, *J. Mater. Process. Tech.* **73** (1998) 160.
7. I. BARIM and O. KNACHE, "Thermochemical Properties of Inorganic Substances [M]," (Springer, Berlin Heidelberg New York, 1973), p. 792.

*Received 9 November 2004  
and accepted 4 March 2005*